journal

J. Am. Ceram. Soc., 74 [7] 1639–45 (1991)

Influence of Stress Ratio on the Elevated-Temperature Fatigue of a Silicon Carbide Fiber-Reinforced Silicon Nitride Composite

John W. Holmes*

Ceramic Composites Research Laboratory, Department of Mechanical Engineering, The University of Michigan, Ann Arbor, Michigan 48109–2125

The influence of stress ratio on the tensile fatigue behavior of a unidirectional SiC-fiber/Si_3N_4-matrix composite was investigated at 1200°C. Tensile stress ratios of 0.1, 0.3, and 0.5 were examined. Fatigue testing was conducted in air, at a sinusoidal loading frequency of 10 Hz. For peak fatigue stresses below the proportional limit of the composite (approximately 195 MPa at 1200°C) specimens survived 5×10^6 cycles, independent of stress ratio. At peak stresses above the proportional limit, fatigue failures were observed; fatigue life decreased significantly as the stress ratio was lowered from 0.5 to 0.1. Creep appears to be the predominant damage mechanism which occurs during fatigue below the proportional limit. Both mechanical cycle-by-cycle fatigue damage and creep contribute to specimen failure at peak stresses above the proportional limit. [Key words: composites, hot pressing, fatigue, creep, silicon nitride.]

I. Introduction

Only a limited number of studies have addressed the fatigue behavior of fiber-reinforced ceramics.[1–9] The lack of this information makes the integration of ceramic-matrix composites into engineering designs difficult. Furthermore, the lack of basic mechanical property data, under various loading histories and temperatures, slows the development of theoretical models required for a basic understanding of the mechanical behavior of fiber-reinforced ceramics.

The occurrence of mechanical, cycle-by-cycle, fatigue damage has been documented in a variety of monolithic[10–30] and whisker-reinforced ceramics.[31,32] Under cyclic loading, failure of monolithic and whisker-reinforced ceramics can occur at applied loads or stress intensities far below those which would cause subcritical crack growth under static loading.[11,16,17,31,32] Fiber-reinforced ceramic composites have also been found to be susceptible to mechanical fatigue damage at ambient[1,4,8] and elevated temperatures.[2,3,5,9] Very little is currently known about the influence of loading history on the elevated-temperature fatigue of ceramic-matrix composites.

Holmes *et al.*[5] recently investigated the influence of maximum fatigue stress on the fatigue life of unidirectional hot-pressed SiC-fiber/Si_3N_4-matrix composites* at 1000°C. It was found that the stress level at which nonlinear behavior began during monotonic tensile loading was an important indicator of the maximum fatigue stress which could be applied without premature fatigue failure. The purpose of the present investigation is to extend this previous work to a temperature range where creep deformation becomes important, and to determine the influence of mean stress ($(\sigma_{max} + \sigma_{min})/2$) on the fatigue life of HP-SiC_f/Si_3N_4 composites.

II. Experimental Procedure

(1) Material and Specimen Geometry

The unidirectional composite used in this investigation consisted of 30 vol% SCS-6 SiC fibers in a Si_3N_4 matrix.† The composite was manufactured by hot-pressing of dry-powder fiber/matrix lay-ups. Hot-pressing was performed at 1700°C under an applied pressure of 70 MPa. The consolidated billets had a density of 3.05 g/mm^3, which is close to 99% of the theoretical density for this composite system. Although axial fiber alignment was within 5° after hot-pressing, fiber spacing was not uniform (see Fig. 1).‡ Porosity was occasionally observed between fibers which were in close proximity to one another.

An edge-loaded specimen geometry (Fig. 2) was used for all monotonic tensile, fatigue, and creep experiments. The overall specimen length was 127 mm, with a gage length of 33 mm. Compared to the edge-loaded specimen used in an earlier study of fatigue at 1000°C,[5] the specimen used in the present investigation had a longer transition length between the gage section and grips. The longer transition length increased the grip-to-grip distance, thereby reducing the temperature gradient developed in the gage section.

(2) Experimental Arrangement

All mechanical testing (monotonic tension, fatigue, and creep) was conducted on a servohydraulic load frame equipped with self-aligning hydraulic grips.§ The experimental arrangement is shown in Fig. 3. An induction-heated SiC susceptor was used to heat the specimen gage section. The length of the furnace hot zone was 65 mm. Although a large temperature gradient exists between the Ni-base grip attachments and specimen gage section, it was possible (through furnace and specimen design) to obtain a uniform gage section temperature. At 1200°C, the maximum temperature difference between any two points along the gage section was approximately 12°C; at a given point, the time variation of temperature was controlled to within ±1°C. The edge-loaded specimen geometry and self-aligning grips provided very accurate and reproducible specimen alignment. For applied stresses above 50 MPa, the bending strain imposed on the specimen through misalignment of the load train was less than 2% of the applied axial strain (bending strains were determined at 22°C in accordance with ASTM Standard E1012-88[36]).

Two contact-type extensometers, located on opposite sides of the specimen, were used to measure gage-section displace-

D. S. Wilkenson—contributing editor

Manuscript No. 197598. Received April 24, 1990; approved April 4, 1991.
Presented at the 14th Annual Conference on Composites and Advanced Ceramics, Cocoa Beach, FL, January 17, 1990 (Engineering Ceramics Division, Paper No. 96-C-90F).

*Member, American Ceramic Society.

*Hereafter referred to as HP-SiC_f/Si_3N_4.

†Material processed by Textron Specialty Materials, Lowell, MA.

‡Other processing techniques, such as tape-casting[33] and reaction bonding,[34,35] have been shown to provide composites with more uniform fiber spacing.

§Model 810, MTS Systems Corporation, Minneapolis, MN.

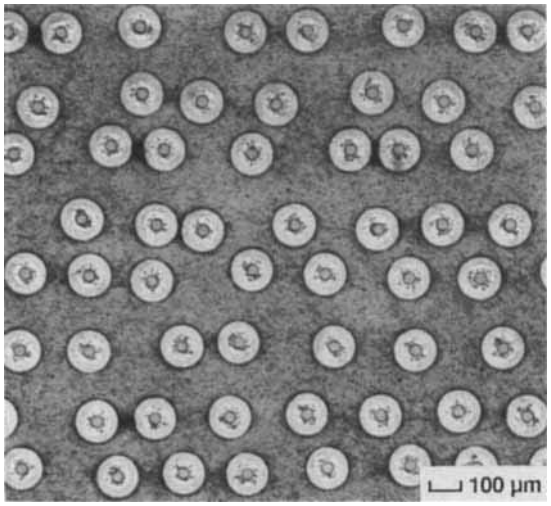

Fig. 1. SEM micrograph showing the typical fiber distribution present in the unidirectional HP-SiC_f/Si_3N_4 specimens. The SCS-6 SiC fibers have a nominal diameter of 142 μm.

ments. The tips of the Al_2O_3 extensometer rods contacted shallow conical dimples which were ground into the edge of the specimens. As discussed by Holmes *et al.*,[5] this counteracting extensometer arrangement allows a moderate extensometer contact force to be used without introducing a net bending force in the specimen (using this extensometer arrangement, transverse loading of the specimen by one extensometer is balanced by equal transverse loading from the opposing extensometer). In the present study, an extensometer contact force of 150 g per rod was employed. A moderate extensometer contact force is beneficial when testing above the proportional limit of fiber-reinforced ceramics, where the energy expended during fracture of the matrix and fibers might otherwise cause extensometer slip. The extensometer and load cell signals were gathered using a data acquisition system with 16-bit resolution and a sampling rate of 10 000

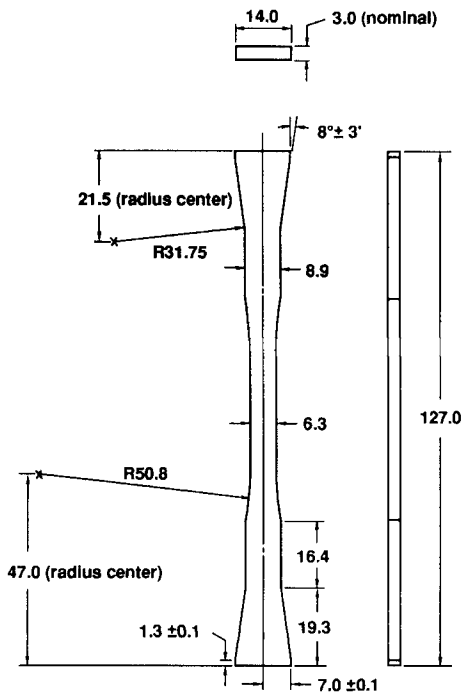

Fig. 2. Edge-loaded specimen used to investigate the monotonic tension, tensile fatigue, and tensile creep behavior of HP-SiC_f/Si_3N_4 composites. (Dimensions in millimeters.)

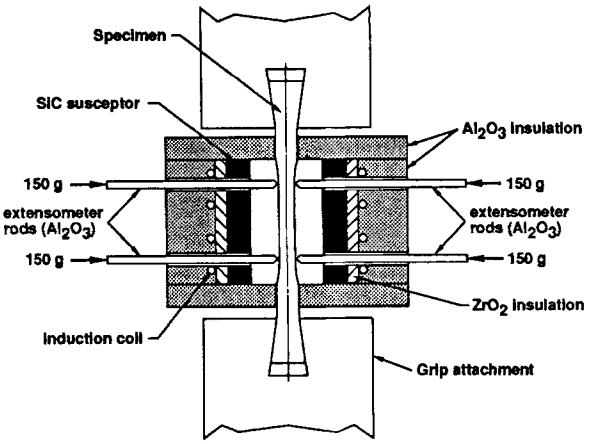

Fig. 3. Schematic of the experimental arrangement used to study the fatigue and creep behavior of HP-SiC_f/Si_3N_4 composites. The use of two extensometers, located on opposite sides of the specimen, allowed using a high contact force without imposing a net bending moment in the specimen.

data points per second.[¶] Initial fatigue data (to 10 000 cycles) were stored at 100-cycle intervals, after which data were typically stored at 1000-cycle intervals.

(3) Test Parameters

To establish the appropriate stress levels for use in the fatigue experiments, the monotonic tensile behavior of the composite was investigated at 1200°C. Tensile testing was conducted in air at a constant loading rate of 100 MPa/s. As shown in Fig. 4, the composite exhibits an initially linear stress–strain response, followed by a gradual decrease in modulus. For purposes of this study, the initial deviation from linearity was defined as the proportional limit strength, σ_{pl}. Based upon four test results, the proportional limit strength of the HP-SiC_f/Si_3N_4 composite used in the present investigation was between 188 and 215 MPa, with an average value of 196 MPa.

All fatigue experiments were performed under load control at a sinusoidal loading frequency of 10 Hz. The fatigue tests were conducted at peak stresses of 180, 200, 220, 240, and 270 MPa (these stresses range from 92% to 140% of the average proportional limit strength at 1200°C). At peak stress of 180 and 270 MPa, stress ratios ($\sigma_{min}/\sigma_{max}$) of 0.1, 0.3, and 0.5

[¶]Model MBC-625 with 16-bit 50 kHz daughterboards, GW Instruments, Sommerville, MA.

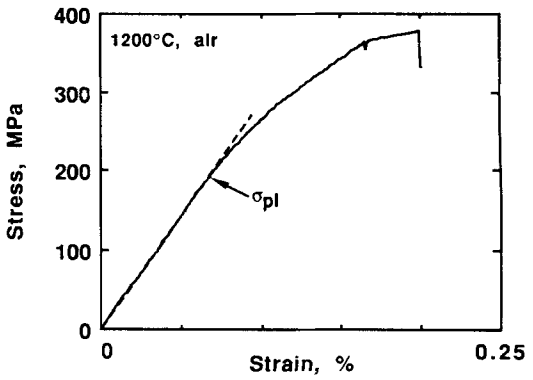

Fig. 4. Typical monotonic tensile curve for HP-SiC_f/Si_3N_4 at 1200°C. Based upon four test results, the initial deviation from linear response occurred between 188 and 215 MPa (defined as the proportional limit strength, σ_{pl}). The average initial tensile modulus was 284 GPa. Tensile testing was conducted at a constant loading rate of 100 MPa/s.

were examined. For all other stresses, testing was limited to stress ratios of 0.1 and 0.5. The fatigue specimens were loaded at a rate of 100 MPa/s to the desired peak stress, followed immediately by cyclic loading (the loading ramp was incorporated to determine the initial tensile behavior of each specimen). Depending upon the scatter observed in the fatigue-life data, three to four specimens were tested for each loading history. Fatigue runout was arbitrarily defined as 5×10^6 cycles, which corresponds to approximately 139 h of testing.

III. Results and Discussion

(1) Tensile Behavior

As noted earlier, at 1200°C the HP-SiC_f/Si_3N_4 composite exhibited a linear stress–strain response up to a stress of approximately 188 to 215 MPa, followed by a gradual decrease in stiffness (Fig. 4). The ultimate strength ranged from 365 to 392 MPa. In all cases, the strain to failure was less than 0.25%. From analysis of the monotonic loading curves, the initial tensile modulus of the composite was between 272 and 290 GPa (the average modulus was 284 GPa). Using data obtained by DiCarlo[37,38] for the 1200°C tensile modulus of SCS-6 SiC fibers, and the dynamic modulus determined by Kossowsky *et al.*[39] for hot-pressed Si_3N_4, a simple rule-of-mixtures calculation predicts an initial modulus of 305 GPa, in good agreement with the average tensile modulus of 284 GPa which was experimentally determined. As verified by surface replicas obtained from a specimen which was sequentially loaded and unloaded in 20-MPa steps (from 140 to 220 MPa), the decrease in modulus which occurs above the proportional limit is associated with the development of several well-defined matrix cracks (at a loading rate of 100 MPa/s, creep deformation does not significantly influence the initial modulus or shape of the monotonic tensile curve[40]).

(2) Fatigue Life and Cyclic Stress–Strain Behavior

(A) $\sigma_{max} < \sigma_{pl}$: At a peak fatigue stress of 180 MPa ($\approx 0.92\sigma_{pl}$) all specimens survived 5×10^6 cycles (139 h at 1200°C), independent of stress ratio (Fig. 5). As shown in Figs. 6(A) and (B), the cyclic stress–strain behavior of the composite remained linear to 5×10^6 cycles, with less than a 5% decrease in modulus found after 5×10^6 cycles. The absence of measurable hysteresis in the cyclic stress–strain response suggests that little, if any, microcracking or fiber fracture occurred during fatigue at stress levels below the proportional limit (significant microstructural damage, in the form of microcracking or fiber fracture, typically causes hysteresis in the cyclic stress–strain response of fiber-reinforced ceramics).[1-3,5-7,41]

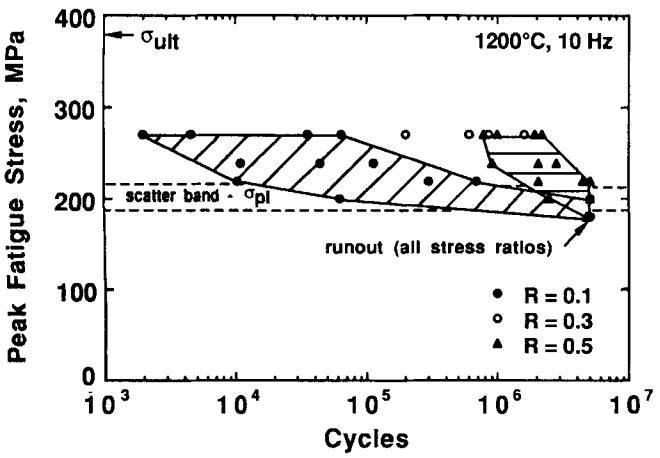

Fig. 5. Influence of stress ratio on the tensile fatigue life of unidirectional HP-SiC_f/Si_3N_4. At 180 MPa all specimens survived 5×10^6 cycles, independent of stress ratio (four specimens were fatigued at each stress ratio). Above the proportional limit, progressive fatigue failures were observed.

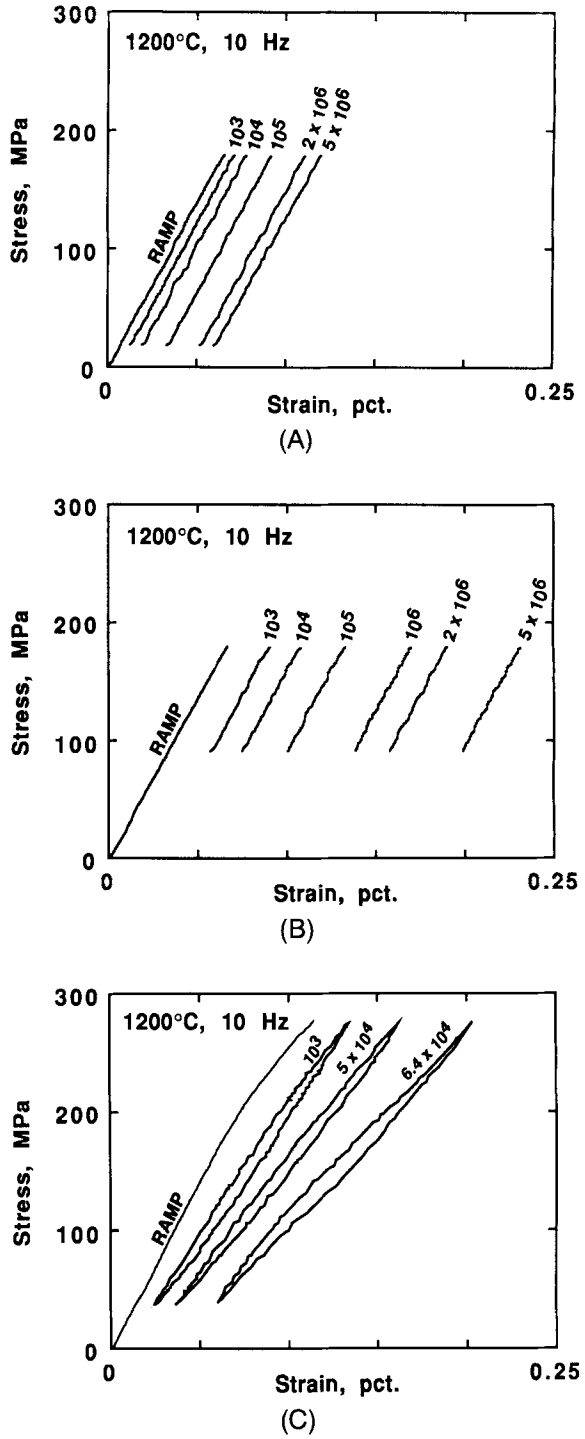

Fig. 6. Cyclic stress–strain behavior of HP-SiC_f/Si_3N_4 at maximum stress levels above and below the monotonic proportional limit ($\sigma_{pl} \approx 196$ MPa); (A) $\sigma_{max} = 180$ MPa, $R = 0.1$, $N_f > 5 \times 10^6$ cycles; (B) $\sigma_{max} = 180$ MPa, $R = 0.5$, $N_f > 5 \times 10^6$ cycles; (C) $\sigma_{max} = 270$ MPa, $R = 0.1$, $N_f = 6.5 \times 10^4$ cycles. Strain ratchetting below the proportional limit ((A) and (B)) is attributed to creep deformation under a tensile mean stress. Above the proportional limit (C), both creep and the accumulation of mechanical fatigue damage contribute to strain ratchetting. The fatigue cycles are given above each curve.

(B) $\sigma_{max} > \sigma_{pl}$: Progressive fatigue failures were observed for maximum fatigue stresses above the proportional limit. The fatigue life of the composite decreased as the stress ratio was lowered from 0.5 to 0.1 (Fig. 5). The scatter in fatigue life data increased significantly as the stress ratio was

lowered; the scatter approached 2 orders of magnitude at a peak stress of 270 MPa and stress ratio of 0.1. Hysteresis in the cyclic stress–strain response of the composite and a progressive decrease in stiffness were observed for maximum fatigue stresses above the proportional limit (Fig. 6(C)). The hysteresis, which was most pronounced at a stress ratio of 0.1, increased with an increase in maximum fatigue stress. Above the proportional limit, the extent of fiber pullout observed after fatigue failure generally increased as the cycles to failure increased. For example, at a peak stress of 270 MPa, very little fiber pullout was observed for fatigue failures that occurred in under 10^4 cycles (Fig. 7(A)), whereas, significant fiber pullout accompanied fatigue failures that occurred at greater than 10^6 cycles (Fig. 7(B)). A similar dependence of fiber pullout length on exposure time was found for failures that occurred during sustained load testing (discussed below).

For a fixed maximum stress, the stress amplitude imposed on the specimen increases as the stress ratio is lowered. Thus the reduction in fatigue life at $R = 0.1$ suggests that cyclic crack propagation controls fatigue life at stresses above the proportional limit (note that if creep was the controlling damage mechanism one would expect an increase in time to failure as the stress ratio, and hence mean stress, is lowered; as discussed later, the opposite trend was found). Although the precise mechanisms which give rise to crack growth during tension–tension fatigue of fiber-reinforced ceramics are not known at this time, it is possible (at elevated temperatures) that cyclic creep in the vicinity of a matrix crack could accelerate crack growth through the formation of a residual tensile zone at the crack tip.

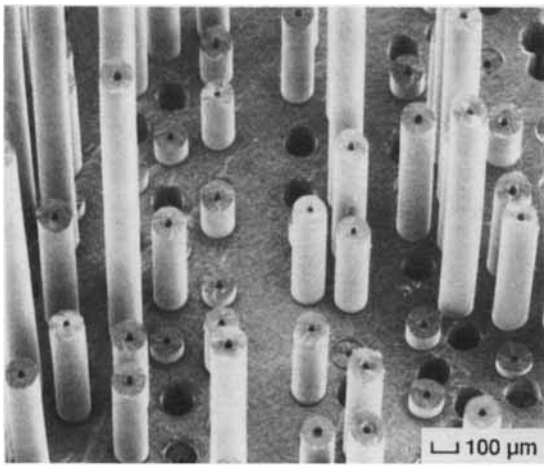

Fig. 7. SEM micrographs comparing the extent of fiber pullout observed for long- and short-duration fatigue loading above the proportional limit; (A) $\sigma_{max} = 270$ MPa ($R = 0.5$), $N_f = 2.2 \times 10^6$ cycles; (B) $\sigma_{max} = 270$ MPa ($R = 0.1$), $N_f = 3.6 \times 10^4$ cycles. At $\sigma_{max} = 270$ MPa, the maximum pullout length was approximately 2.8 mm ($R = 0.5$) and 0.9 mm ($R = 0.1$). The fiber core (carbon) was partially oxidized during cooldown of the furnace after specimen failure.

(3) Role of Creep Deformation

(A) $\sigma_{max} < \sigma_{pl}$: Although stress–strain hysteresis was not observed during fatigue at maximum stresses below σ_{pl}, a significant amount of strain ratchetting** was found (see Figs. 6(A) and (B)). The extent of strain ratchetting increased significantly as the stress ratio was increased from 0.1 to 0.5. In an effort to understand the mechanisms responsible for this strain ratchetting, a series of creep tests were conducted at stress levels equal to the mean stress employed in fatigue testing. The results obtained from creep tests conducted at 99 MPa are given in Fig. 8 (99 MPa is equal to the mean stress for fatigue at $\sigma_{max} = 180$ MPa and $R = 0.1$). Also shown in Fig. 8 is the increase in specimen strain measured during fatigue.†† Although the initial strain rate was much higher for fatigue loading, the steady-state increase in strain (defined here as the apparent steady-state creep rate) was similar for both creep and fatigue loading (see Fig. 9). At 99 MPa the apparent steady-state creep rate ranged from an average of 9×10^{-11} s^{-1} for creep loading to 2×10^{-10} s^{-1} for fatigue loading. As the stress ratio was increased from 0.1 to 0.5, the correlation between the steady-state creep rate for sustained and cyclic loading improved (this is to be expected, however, since a limiting stress ratio of 1.0 would correspond to a static load test). Fitting the steady-state creep rate data given in Fig. 9 to a simple power-law relation between creep rate and applied stress ($\dot{\varepsilon}_{ss} = B\sigma^m$) yields a stress exponent of approximately 6.0. A similar analysis of the strain ratchetting found for fatigue loading gives a stress exponent of 5.7. The similarity in stress exponents found for creep and fatigue loading

**Note that strain ratchetting refers to the time-dependent progression of the cyclic stress–strain curves along the strain axis.

††The specimen strain plotted in Fig. 8 was taken at the mean stress level. Since the cyclic stress–strain curves were linear for maximum fatigue stresses below the proportional limit (Fig. 6(A)), using a different value of strain (e.g., that corresponding to the maximum fatigue stress) would translate the "creep" curves vertically along the strain axis, but would not alter their slope.

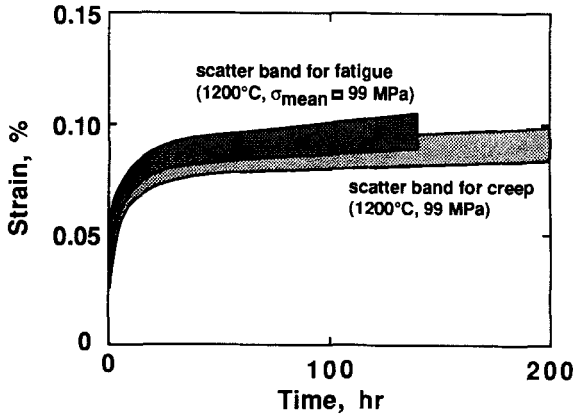

Fig. 8. Comparison of creep deformation under static loading with the strain ratchetting found during fatigue at a maximum stress below the proportional limit. The creep tests were conducted at a stress level of 99 MPa, which is equal to the mean stress for fatigue at $\sigma_{max} = 180$ MPa and $R = 0.1$. The shaded scatter bands represent best fits to the maximum and minimum curves found for creep and fatigue loading.

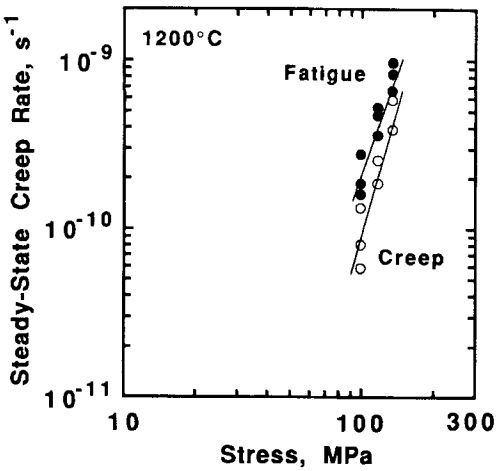

Fig. 9. Comparison of the apparent steady-state creep rate for fatigue and creep loading. The fatigue data shown were obtained at peak stresses *below* the proportional limit.

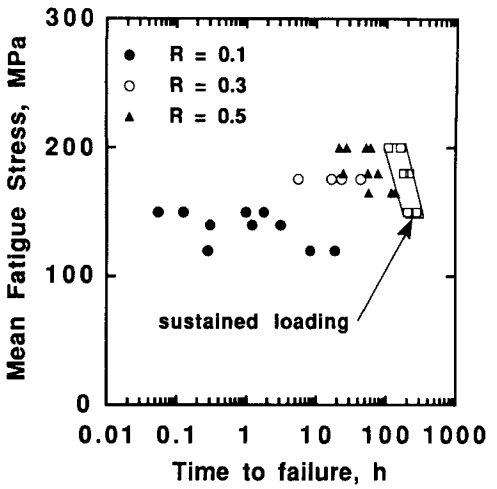

Fig. 10. Comparison of failure times for sustained and fatigue loading. The fatigue data shown were obtained from experiments conducted at maximum stress levels of 220, 240, and 270 MPa (these stress levels are above the initial monotonic proportional limit strength of the composite).

suggests that the damage mechanism is similar for these two loading histories. The results indicate that the strain ratchetting observed during fatigue below σ_{pl} was caused primarily by time-dependent creep deformation under a tensile mean stress, rather than cycle-by-cycle crack growth (note that cyclic crack growth or an increase in crack density would significantly reduce composite stiffness—which was not observed). Thus, below the proportional limit and for positive stress ratios, creep appears to be the primary damage mechanism which occurs in HP-SiC_f/Si_3N_4 composites.

(B) $\sigma_{max} > \sigma_{pl}$*:* For fatigue loading at a maximum stress above the initial proportional limit, both cycle-by-cycle (mechanical) fatigue crack growth and crack growth by creep are possible. In addition to the direct growth of matrix or interfacial cracks by creep, creep deformation will alter the residual stress state which exists in the composite. This is important, since a change in residual stress state will directly influence the rate of crack growth. One consequence of creep deformation is a shift in the average matrix stress to a more positive value; creep of the matrix can also alter the interfacial shear which exists along the fiber/matrix interface.[42] Thus, the extent of microstructural damage which occurs during elevated temperature cyclic loading will be intimately related to the creep rates of the fiber and matrix.

To determine if creep deformation played a significant role in determining specimen life during fatigue at peak stresses above the proportional limit, the failure times for sustained loading (stress rupture) and fatigue loading were compared. Based upon the correlation found above for the creep rates under sustained loading and cyclic loading below the proportional limit (Fig. 9), the mean fatigue stress was used for the comparison of failure times. The sustained-load experiments were conducted at stresses of 150, 175, and 200 MPa. These stresses are approximately equal to the mean fatigue stress which would have been present during fatigue at a maximum stress of 270 MPa and stress ratios of 0.1, 0.3, and 0.5. To simulate the *initial* microstructural damage that would be present in the fatigue experiments, the creep specimens were first loaded to 270 MPa at a rate of 100 MPa/s, followed by constant loading at the desired creep stress.

When plotted against the mean stress, the failure times for fatigue loading are found to be lower than those for sustained loading. For example, the failure time exceeded 200 h for sustained loading at a stress of 150 MPa, whereas failure times for fatigue at a mean stress of 150 MPa ($R = 0.1$) were under 2 h. The large difference in failure times for sustained and fatigue loading at a stress ratio of 0.1 offers evidence that mechanical cycle-by-cycle fatigue damage accelerates the accumulation of microstructural damage for stresses above the proportional limit. The occurrence of cyclic damage can also be inferred from the rapid decrease in specimen stiffness which was found for peak stresses above the proportional limit (Fig. 6(C)). For a stress ratio of 0.5, the failure times for creep and fatigue loading did not differ substantially (Fig. 10); these results suggest that creep, rather than cycle-by-cycle fatigue damage, may be the controlling damage mechanism which occurs under a high mean stress.

It is important to note that the comparison of failure times was made using the mean fatigue stress. However, in view of the high stress sensitivity of creep (as discussed earlier, the stress exponent for creep is approximately 6), substantial creep deformation can occur during the portion of the fatigue cycle which is above the mean stress. Thus, although plotting the rupture times for fatigue against the mean fatigue stress provides a convenient approach for judging the influence of stress ratio on rupture time, it may seriously overestimate the stress sensitivity of failure time.

As noted earlier, Han and Suresh[32] found that the rate of cyclic crack growth in SiC_w/Al_2O_3 composites tested at 1400°C *decreased* as the stress ratio was lowered. In the present investigation, it was found that for peak stresses above the proportional limit the fatigue life of HP-SiC_f/Si_3N_4 composites decreased as the stress ratio was lowered. Since fatigue life should roughly scale with the rate of crack propagation, the results obtained in the present investigation suggest that the rate of crack propagation in HP-SiC_f/Si_3N_4 composites *increases* as the stress ratio is lowered. The different manner in which stress ratio influences the fatigue behavior of SiC_w/Al_2O_3 and HP-SiC_f/Si_3N_4 composites may be a reflection of the different creep strengths of these two systems (note also that the SiC_w/Al_2O_3 composite was investigated at a temperature where the creep rate of the Al_2O_3 matrix would be rapid). In general, elevated-temperature fatigue life of a ceramic composite will depend upon the competing effects of mechanical cycle-by-cycle crack growth and crack growth caused by matrix creep. Both modes of crack growth will be strongly influenced by the change in the residual stress state which occurs during cyclic loading. For a given temperature, the residual stress state which develops in the composite will be governed by the relative creep rates of the fiber and matrix. Moreover, both fiber architecture and interfacial properties will influence the ability of a particular composite microstructure to arrest crack propagation under creep-fatigue loading. In view of the competing effects of fiber and matrix creep, fiber architecture, and interfacial properties, and the scarcity of data concerning the creep or

fatigue behavior of other fiber-reinforced ceramics, it is difficult to predict if the trends observed in the present investigation will apply for other fiber-reinforced ceramics.

(4) Influence of Fatigue on Tensile Behavior

Monotonic tensile testing of four specimens which had been fatigued for 5×10^6 cycles at a peak stress below the proportional limit was conducted to determine the effect of long-duration cyclic loading on the composite modulus, ultimate strength, and proportional limit. To avoid further changes in microstructure or internal stress state of the composite, the tensile tests were conducted immediately after completion of each fatigue test. The results of these tensile tests showed that a decrease in both composite modulus (<5%) and ultimate strength (<20% reduction) occurred as a consequence of fatigue loading (see Fig. 11). Interestingly, the proportional limit strength increased after fatigue loading; the proportional limit strength ranged from 242 to 280 MPa (for as-received material, the proportional limit ranged from 188 to 215 MPa).

In a recent investigation of the monotonic tensile behavior of unidirectional HP-SiC_f/Si_3N_4 composites it was found that isothermal exposure at 1200°C for 200 h (without load) decreased the ultimate strength by approximately 10% and slightly decreased the proportional limit strength.[40] These results suggest that the increase in proportional limit strength which occurred after cyclic loading was caused by deformation-related phenomena, such as a change in the residual stress state of the composite, rather than a change in interfacial properties acting alone. One plausible mechanism is a change in the residual stress state in the composite caused by cyclic creep of the matrix. Upon cooling of the composite billets from the processing temperature (1700°C) to room temperature, the matrix is placed in a state of residual compression parallel to the fiber axis (note that the thermal expansion coefficient of the matrix is less than that of the fiber). Although reduced in magnitude (because of the smaller temperature difference), residual compression will persist after heating a virgin test specimen to 1200°C. Through finite element calculations, Park and Holmes[42] have estimated that a compressive matrix stress of approximately 100 MPa would be present in a virgin HP-SiC_f/Si_3N_4 tensile specimen which is heated without loading to 1200°C (this estimate assumes perfect bonding along the fiber/matrix interface; the initial compressive stress would be much lower if debonding occurs during processing of the billets). During subsequent fatigue at 1200°C, cyclic creep of the matrix relaxes the matrix stress through the transfer of load to the fibers. For long-duration cyclic loading, the mean stress acting in the matrix can approach zero. However, maintaining the specimen temperature at 1200°C, and reducing the fatigue load to zero (as in the present investigation) places the matrix in a state of residual compression by elastic contraction of the fibers. Finite element studies of tensile-creep deformation in HP-SiC_f/Si_3N_4 composites at 1200°C, show that the magnitude of the compressive stress which exists immediately after specimen unloading is *larger* than the processing-related residual stress which would be present in a virgin specimen heated to 1200°C. Thus, compared to as-processed specimens, a larger external stress must be applied to the fatigue specimens to achieve a net tensile stress in the matrix sufficient to initiate cracking, leading to a higher apparent proportional limit strength.

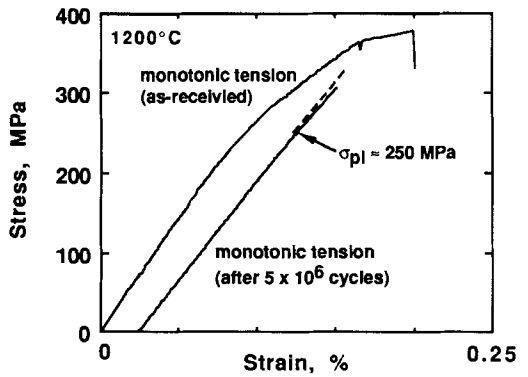

Fig. 11. Influence of long-duration fatigue loading below the proportional limit on the monotonic tensile behavior of HP-SiC_f/Si_3N_4. The curve to the right was obtained from a specimen which had been subjected to 5×10^6 cycles at a peak stress of 180 MPa and stress ratio of 0.1 (the approximately linear stress–strain response shown above is representative of that found for other specimens fatigued below the proportional limit). After fatigue, the proportional limit increased by approximately 20–35%, and the ultimate strength decreased by 12–20%.

It was of interest to determine if the higher proportional limit strength found after long-duration fatigue at peak stresses below the initial proportional limit would shift the fatigue limit to higher stresses. To study this possibility, two specimens, which had undergone 5×10^6 fatigue cycles at a peak stress of 180 MPa ($R = 0.1$), were subjected to fatigue at a peak stress of 240 MPa ($R = 0.1$). These specimens failed between 2.1×10^6 and 3.2×10^6 cycles; as-received samples that were fatigued under similar loading conditions survived only 2000 to 50 000 cycles. These results clearly illustrate the influence of matrix cracking on the elevated temperature fatigue life of HP-SiC_f/Si_3N_4 composites. Although the fatigue limit of the composite increased after prolonged fatigue below the initial proportional limit, this result must be viewed with caution, since the ultimate strength and toughness of the composite can decrease after elevated temperature exposure (Fig. 11).

IV. Summary

Based upon results obtained from tension–tension fatigue and tensile-creep testing of unidirectional hot-pressed SiC_f/Si_3N_4 composites at 1200°C, the following comments can be made:

(1) For peak fatigue stresses below the monotonic proportional limit (≈196 MPa), fatigue runout at 5×10^6 cycles was observed for tensile stress ratios between 0.1 and 0.5. For a fixed maximum fatigue stress above the proportional limit, fatigue life decreased as the stress amplitude was increased. At a stress ratio of 0.1, failure times under fatigue loading were significantly shorter than the failure times found for sustained loading at stress levels equal to the mean fatigue stress.

(2) Strain ratchetting was observed during fatigue at maximum stresses above and below the monotonic proportional limit. Below the proportional limit, the rate of strain ratchetting was similar to the creep rate measured during static-load experiments conducted at stress levels equal to the mean fatigue stress. Based upon this correlation, creep appears to be the predominate damage mechanism which occurs during elevated temperature cyclic loading below the monotonic proportional limit. Above the proportional limit, both creep damage and mechanical fatigue damage contribute to strain ratchetting.

(3) Long-term fatigue loading below the proportional limit resulted in a 20–35% increase in the monotonic proportional limit and approximately a 20% decrease in ultimate strength. The change in tensile behavior is attributed to a change in the residual stress state of the composite caused by long-term elevated temperature exposure under a tensile mean stress.

(4) Insufficient data are available to determine if the trends in elevated temperature fatigue behavior which were observed in the present investigation can be extrapolated to other, more complicated composite microstructures.

Acknowledgment: The author would like to express his appreciation to Textron Specialty Materials for supplying the hot-pressed SiC_f/Si_3N_4 used in this investigation.

References

[1]E. Minford and K. M. Prewo, "Fatigue of Silicon Carbide Reinforced Lithium-Alumino-Silicate Glass-Ceramics"; pp. 561–70 in *Tailoring Multiphase and Composite Ceramics.* Edited by C. G. Patano and R. E. Messing. Plenum Press, New York, 1986.

[2]K. M. Prewo, "Fatigue and Stress Rupture of Silicon Carbide Fibre-Reinforced Glass Ceramics," *J. Mater. Sci.*, **22**, 2695–701 (1987).

[3]K. M. Prewo, B. Johnson, and S. Starrett, "Silicon Carbide Fiber-Reinforced Glass Ceramic Composite Tensile Behavior at Elevated Temperature," *J. Mater. Sci.*, **24**, 1373–79 (1989).

[4]H. Sakamoto, K. Hironori, and T. Miyoshi, "In Situ Observation of Fracture Behavior of SiC Fiber–Si_3N_4 Matrix Composite," *J. Ceram. Soc. Jpn. (Int. Ed.)*, **95**, 817–22 (1987).

[5]J. W. Holmes, T. Kotil, and W. T. Foulds, "High Temperature Fatigue of SiC Fiber Reinforced Si_3N_4 Ceramic Composites"; pp. 176–82 in Symposium on High Temperature Composites. Technomic Publishing Company, Lancaster, PA (1989).

[6]T. Kotil, J. W. Holmes, and M. Comninou, "The Origin of Hysteresis During Cyclic Loading of Ceramic Matrix Composites," *J. Am. Ceram. Soc.*, **73** [7] 1879–83 (1990).

[7]J. W. Holmes and S. F. Shuler, "Temperature Rise During Fatigue of Fiber-Reinforced Ceramics," *J. Mater. Sci. Lett.*, **9**, 1290–91 (1990).

[8]E. Y. Luh, R. H. Dauskardt, and R. O. Ritchie, "Cyclic Fatigue-Crack Growth Behavior of Short Cracks in SiC-Reinforced LAS Glass-Ceramic Composite," *J. Mater. Sci. Lett.*, **9**, 719–25 (1990).

[9]C. Q. Rousseau, "Monotonic and Cyclic Behavior of a Silicon Carbide/Calcium-Aluminosilicate Ceramic Composite"; in *Thermal and Mechanical Behavior of Metal Matrix and Ceramic Matrix Composites,* ASTM STP 1080. Edited by J. M. Kennedy, H. H. Moeller, and W. S. Johnson. American Society for Testing and Materials, Philadelphia, PA, 1990, in press.

[10]R. H. Dauskardt, W. Yu, and R. O. Ritchie, "Fatigue Crack Propagation in Transformation-Toughened Zirconia Ceramic," *J. Am. Ceram. Soc.*, **70** [10] C-248–C-252 (1987).

[11]R. H. Dauskardt, D. B. Marshall, and R. O. Ritchie, "Cyclic Fatigue Crack Propagation in Magnesia-Partially-Stabilized Zirconia Ceramics," *J. Am. Ceram. Soc.*, **23** [4] 893–903 (1990).

[12]K. J. Bowman, P. E. Reyes-Morel, and I-W. Chen, "Reversible Transformation Plasticity in Uniaxial Tension-Compression Cycling of Mg-PSZ"; in *Advanced Structural Ceramics,* MRS Symposium Proceedings: Edited by P. F. Becher, M. V. Swain, and S. Somiya. Materials Research Society, Pittsburgh, PA, 1986.

[13]W. Liu and I-W. Chen, "Fatigue of Yttria-Stabilized Zirconia I: Fatigue Damage, Fracture Origins and Lifetime Prediction," *J. Am. Ceram. Soc.*, in press.

[14]W. Liu and I-W. Chen, "Fatigue of Yttria-Stabilized Zirconia II: Crack Propagation, Fatigue Striations and Short Crack Behavior," *J. Am. Ceram. Soc.*, in press.

[15]A. G. Evans, "Fatigue in Ceramics," *Int. J. Fract.*, **16** [10] 485–98 (1980).

[16]A. G. Evans and M. Linzer, "High Frequency Cyclic Crack Propagation in Ceramic Materials," *Int. J. Fract.*, **12** [2] 217–22 (1976).

[17]L. E. Ewart and S. Suresh, "Dynamic Fatigue Crack Growth in Polycrystalline Alumina under Cyclic Compression," *J. Mater. Sci. Lett.*, **4**, 774–78 (1986).

[18]L. E. Ewart and S. Suresh, "Crack Propagation in Ceramics under Cyclic Loads," *J. Mater. Sci.*, **22**, 1173–92 (1987).

[19]D. A. J. Vaughan and F. Guiu, "Cyclic Fatigue of Advanced Ceramics," *Proc. Br. Ceram. Soc.*, **39**, 101–108 (1987).

[20]A. A. Steffen, R. H. Dauskardt, and R. O. Ritchie, "Cyclic Fatigue-Crack Propagation in Ceramics: Long and Small Crack Behavior"; pp. 745–52 in FATIGUE 90, Proceedings of the Fourth International Conference on Fatigue and Fatigue Thresholds, Honolulu, Hawaii. Edited by H. Kitagawa and T. Tanaka. Materials and Component Engineering Publications Ltd., Birmingham, U.K., 1990.

[21]L. S. Williams, "Stress-Endurance of Sintered Alumina," *Trans. Br. Ceram. Soc.*, **55** [5] 287–312 (1956).

[22]L. S. Williams; Ch. 18 in *Mechanical Properties of Engineering Ceramics.* Edited by W. W. Kriegel and H. Palmour. Interscience, New York, 1961.

[23]A. Grossmuller, V. Zelizko, and M. V. Swain, "Fatigue Crack Growth in Ceramics Using a Compressive Loading Geometry," *J. Mater. Sci. Lett.*, **8**, 29–31 (1989).

[24]F. Guiu, "Cyclic Fatigue of Polycrystalline Alumina in Direct Push-Pull," *J. Mater. Sci. Lett.*, **13** [6] 1157–361 (1978).

[25]H. N. Ko, "Fatigue Strength of Si_3N_4 under Rotary Bending," *J. Mater. Sci. Lett.*, **5** [2] 175–77 (1987).

[26]D. A. Krohn and D. P. H. Hasselman, "Static and Cyclic Fatigue Behavior of a Polycrystalline Alumina," *J. Am. Ceram. Soc.*, **55** [4] 208–11 (1972).

[27]D. Lewis and R. W. Rice, "Comparison of Static, Cyclic and Thermal Shock Fatigue in Ceramic Composites," *Ceram. Eng. Sci. Proc.*, **3** [9–10] 714–21 (1982).

[28]M. J. Reece, F. Guiu, and M. F. R. Sammur, "Cyclic Fatigue Crack Propagation in Alumina under Direct Tension–Compression Loading," *J. Am. Ceram. Soc.*, **72** [2] 348–52 (1989).

[29]T. Kawakubo and K. Komeya, "Static and Cyclic Fatigue Behavior of a Sintered Silicon Nitride at Room Temperature," *J. Am. Ceram. Soc.*, **70** [6] 400–405 (1987).

[30]S. Suresh and J. R. Brockenbrough, "Theory and Experiments of Fracture in Cyclic Compression; Single Phase Ceramics, Transforming Ceramics and Ceramic Composites," *Acta Metall.*, **36** [6] 1455–70 (1988).

[31]S. Suresh, L. X. Han, and J. J. Petrovic, "Fracture of Si_3N_4–SiC Whisker Composites under Cyclic Loads," *J. Am. Ceram. Soc.*, **71** [3] C-158–C-161 (1988).

[32]L. X. Han and S. Suresh, "High Temperature Failure of an Alumina–Silicon Carbide Composite under Cyclic Loads: Mechanisms of Fatigue Crack-Tip Damage," *J. Am. Ceram. Soc.*, **72** [7] 1233–38 (1989).

[33]J.-F. LeCostaouec, Textron Specialty Materials, Lowell, MA; personal communication, February, 1990.

[34]R. T. Bhatt, "Oxidation Effects on the Mechanical Properties of SiC Fiber-Reinforced Reaction-Bonded Silicon Nitride Matrix Composites," NASA Technical Memorandum 102360. National Aeronautics and Space Administration, Washington, DC, 1989.

[35]R. T. Bhatt, "Laminate Behavior for SiC Fiber-Reinforced Reaction-Bonded Silicon Nitride Matrix Composites," NASA Technical Memorandum 101350. National Aeronautics and Space Administration, Washington, DC, 1988.

[36]ASTM Annual Book of Standards, Vol. 3.01; p. 255. American Society for Testing and Materials, Philadelphia, PA, 1988.

[37]J. A. DiCarlo, "Creep of Chemically Vapour Deposited SiC Fibers," *J. Mater. Sci.*, **21**, 217–24 (1986).

[38]J. A. DiCarlo, "High Temperature Properties of CVD Silicon Carbide Fibers"; presented at the International Conference of Whisker- and Fiber-Toughened Ceramics (Oak Ridge, TN, June 7–9, 1988).

[39]R. Kossowsky, D. G. Miller, and E. S. Diaz, "Tensile and Creep Strengths of Hot-Pressed Si_3N_4," *J. Mater. Sci.*, **10**, 983–97 (1975).

[40]J. W. Holmes, "Tensile and Creep Behavior of Fiber-Reinforced SiC_f/Si_3N_4 Composites"; presented at the 6th Annual ASM/ESD Conference on Advanced Composites (Detroit, MI, October 8–11, 1990).

[41]D. B. Marshall and A. G. Evans, "Failure Mechanisms in Ceramic-Fiber/Ceramic-Matrix Composites," *J. Am. Ceram. Soc.*, **68** [5] 225–31 (1985).

[42]Y. Park and J. W. Holmes, "Finite Element Modelling of the Tensile Creep Behavior of SiC-Fiber Si_3N_4-Matrix Composites," *J. Mater. Sci.*, in review. □